
Reason3D: Searching and Reasoning 3D Segmentation via Large Language Model

Kuan-Chih Huang¹ Xiangtai Li² Lu Qi^{1*} Shuicheng Yan² Ming-Hsuan Yang¹

¹University of California, Merced ²Skywork AI

Abstract

Recent advancements in multimodal large language models (LLMs) have shown their potential in various domains, especially concept reasoning. Despite these developments, applications in understanding 3D environments remain limited. They primarily offer textual or numerical outputs without the capability to generate dense, informative segmentation masks. This paper introduces Reason3D, a novel LLM designed for comprehensive 3D understanding. Reason3D takes point cloud data and text prompts as input to produce textual responses and segmentation masks, facilitating advanced tasks like 3D reasoning segmentation, hierarchical searching, express referring, and question answering with detailed mask outputs. Specifically, we propose a hierarchical mask decoder to locate small objects within expansive scenes. This decoder initially generates a coarse location estimate covering the object’s general area. This foundational estimation facilitates a detailed, coarse-to-fine segmentation strategy that significantly enhances the precision of object identification and segmentation. Experiments validate that Reason3D achieves remarkable results on large-scale ScanNet and Matterport3D datasets for 3D express referring, 3D question answering, and 3D reasoning segmentation tasks. Code and models are available at: <https://github.com/KuanchihHuang/Reason3D>.

1 Introduction

Recently, large language models (LLMs) [41, 42, 20] have significantly enhanced their capabilities in sophisticated reasoning within the realm of natural language processing. Building on these developments, a new class of models, known as Multimodal Large Language Models (MLLMs) [14, 26, 3, 28, 54, 36, 50, 52] have emerged. These models are designed to process multiple modalities, including 2D images [28, 3], thereby enriching LLMs’ ability to interpret and understand visual inputs. However, while MLLMs demonstrate remarkable proficiency with 2D imagery, extending these capabilities to complex 3D environments remains a formidable challenge, which is critical in various technological domains, including robot navigation and embodied AI agents.

Numerous studies have made significant strides in using point clouds as input tokens for 3D large language models (LLMs). Some researches [49, 33, 32, 40] primarily focused on 3D object-level understanding. Prior study 3D-LLM [17] aggregates multi-view features to enrich 3D feature comprehension and employs a subsequent LLM for 3D reasoning. Meanwhile, LL3DA [8] directly encodes 3D point clouds for scene representation and facilitates human interaction to enhance understanding.

These methods integrate large language models (LLMs) with point cloud inputs to enhance 3D reasoning capabilities; however, they also encounter specific limitations. Firstly, the outputs from

*Corresponding author

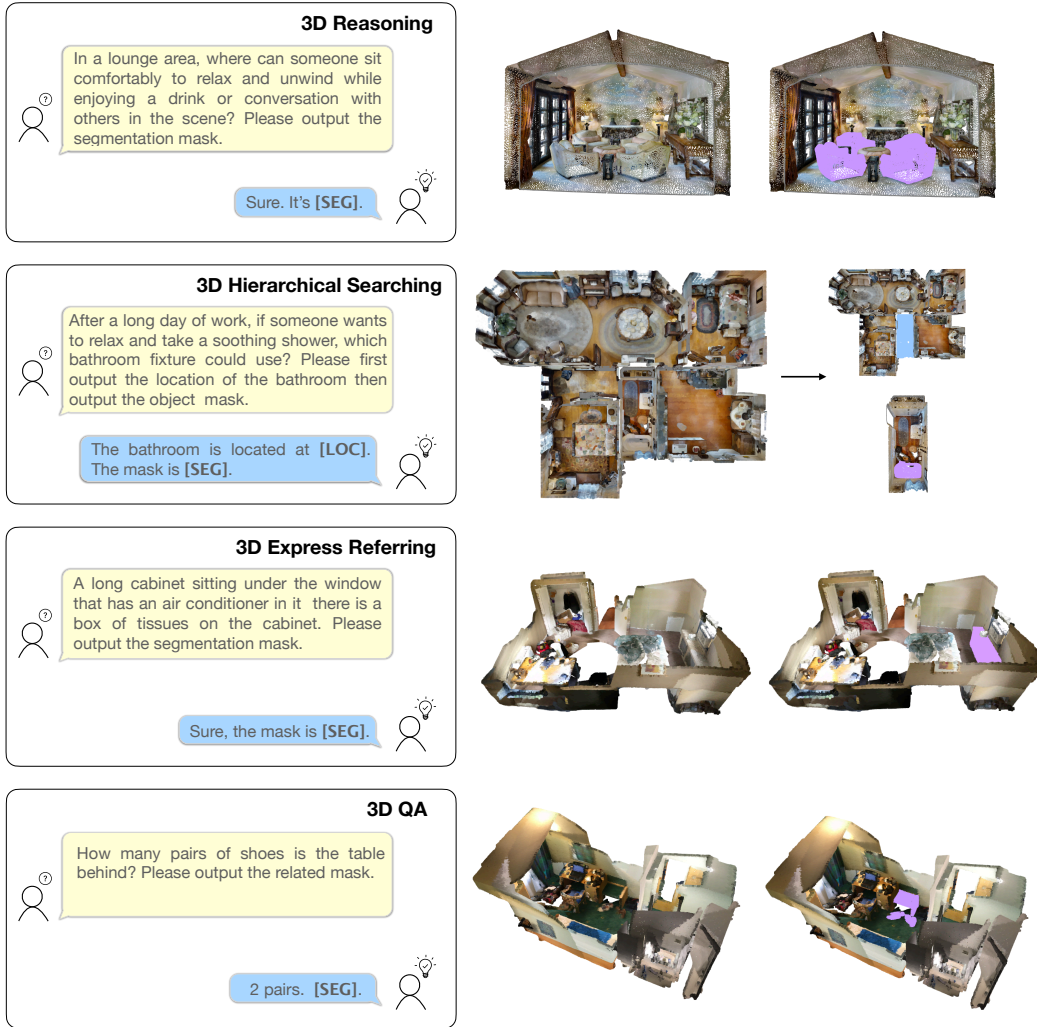


Figure 1: We propose Reason3D, a novel LLM-based dense 3D point cloud searching and reasoning framework that can output dense segmentation masks based on textural information. Our Reason3D can handle tasks involving 1) 3D Reasoning, 2) 3D Hierarchical Searching, 3) 3D express referring, and 4) 3D QA with responding dense segmentation masks.

these models are confined to textual or numerical forms, which are inadequate for predicting dense data types, such as segmentation masks, essential for detailed spatial analysis. Secondly, these models struggle to locate or search for objects in 3D scenes based on complex or abstract concepts rather than relying on spatial relationships within the scenes.

To enable 3D-based LLM models to produce segmentation masks, we can direct the LLM to generate a [SEG] token. The embedding of this token is then utilized to guide the decoder in learning to create 3D segmentation masks, similar to approaches used in 2D reasoning models [24]. However, unlike structured image data, this straightforward adaptation may encounter difficulties due to point clouds' inherent sparsity and unstructured nature. These challenges are particularly pronounced when attempting to output masks for small objects within dense, large-scale 3D scenes.

In this paper, we introduce Reason3D, a framework designed to enable reasoning and searching within 3D scenes using large language models with point cloud inputs. Unlike other methods that generate only textual and numerical outputs, Reason3D also produces 3D segmentation masks from textual inputs. To efficiently manage large-scale point clouds, we utilize a superpoint pooling layer that aggregates data into precomputed superpoints, significantly reducing complexity. Furthermore, we develop a hierarchical mask decoder to address the challenges of sparsity in extensive point clouds, such as locating a ball in a large house. This decoder employs a coarse-to-fine strategy, initially

identifying a likely object-containing coarse region by instructing the LLM model to output a [LOC] embedding, which guides the learning of the region mask. This region then serves as a prior to generate a precise object mask, facilitating effective localization in complex 3D environments.

Figure 1 illustrates Reason3D’s capability to handle diverse scenarios requiring advanced reasoning, searching, and question answering based on conceptual and spatial information. To validate the effectiveness of our approach, we have collected a dataset for 3D reasoning segmentation, comprising over one thousand point-instruction pairs. To ensure this dataset closely mirrors real-world applications, we annotated point clouds from Matterport3D [6] and ScanNetv2 [13] with implicit text queries that demand complex reasoning. The main contributions of this work are:

- We introduce Reason3D, a comprehensive framework for reasoning and searching within 3D scenes using extensive language prompts. This framework not only processes 3D point clouds and language prompts to generate textual outputs but also creates detailed 3D segmentation masks. Reason3D supports a wide range of tasks, including 3D expressive referring segmentation, 3D reasoning segmentation, 3D hierarchical searching, and 3D question answering.
- We establish the novel task of 3D reasoning segmentation, which involves interpreting implicit human instructions within 3D scenes, and build a dataset to evaluate this task. The capability of 3D reasoning is essential for developing truly advanced 3D perception systems.
- We develop a hierarchical mask decoder to address the sparsity of 3D point clouds effectively. This innovative approach first identifies a coarse region likely containing the object and uses this region’s probability as a prior to guide the refinement of the final mask prediction.
- We develop a hierarchical mask decoder to address the sparsity of 3D point clouds effectively. This innovative approach first identifies a coarse region likely containing the object. Then, the decoder uses this region’s probability as a prior to guide the refinement of the final mask prediction.

2 Related Work

3D Point Cloud Segmentation. Recent advancements in point cloud segmentation [31, 23, 38, 48, 37, 44] have driven the evolution of various class-aware prediction techniques, predominantly employing UNet-like models that process data as either 3D points or voxels. Point-based methods [9, 55] refine feature extraction through aggregation mechanisms or transformer blocks, while voxel-based methods [18, 11] transform irregular point clouds into regular voxel grids for processing with dense or sparse 3D convolutional networks, enhancing segmentation accuracy and efficiency. With 3D segmentation tasks having achieved a significant level of maturity, it has become essential to develop more advanced methods for interacting with 3D segmentation systems.

The 3D express referring segmentation task [7, 1] enhances interaction through human language by segmenting a 3D object according to a specific textual description. TGNN [19] employs a two-stage approach that integrates instance and textual features, computing a matching score for each instance to identify the target described in the text. Building on this, X-RefSeg3D [34] leverages vision-language cues by combining entity-related linguistic information with visual features to construct a cross-modal scene graph, which facilitates interactions based on textual and spatial relations. Similarly, 3D-STMN [45] introduces an efficient end-to-end framework that utilizes superpoints and aligns them with textual modalities, thereby enhancing their role in multimodal representation. However, while these studies make significant strides in object identification using spatial relation cues, they do not fully explore deeper reasoning capabilities. In this work, we introduce Reason3D, a novel approach that extends beyond traditional identification to incorporate advanced reasoning with 3D segmentation models, addressing complex interactions not yet tackled by existing methodologies.

Large Language Model. Recent advancements in large language models (LLMs) [41, 57, 42, 20, 21] have showcased their broad generalization across diverse language tasks, thanks to training on extensive textual datasets. Through self-supervised learning techniques such as token prediction and masked token reconstruction, as well as further refinements via instruction tuning and specialized datasets, researchers have significantly enhanced the adaptability of these models to new tasks. Building on this, the remarkable reasoning capabilities of LLMs are increasingly applied in multimodal contexts. Modern models incorporate advanced architectures that integrate visual data [26, 2, 3, 28, 58, 24, 14, 47, 50, 53, 46], utilizing mechanisms such as cross-attention and image-text feature alignment to enable comprehensive multimodal understanding. This has paved the way for models that engage in visual question answering and perform complex reasoning tasks.

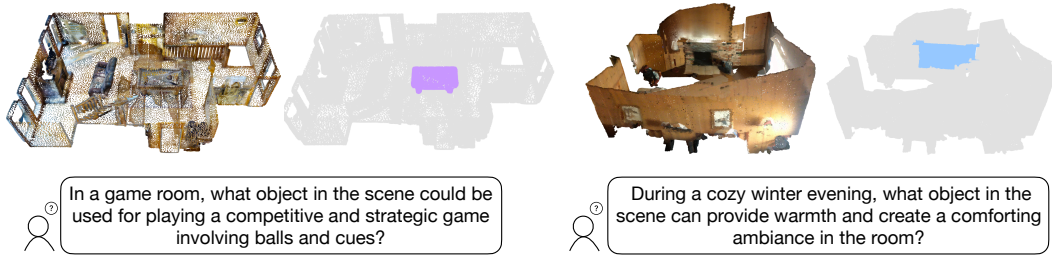


Figure 2: **Examples of the annotated samples.** Left is one data from Matterport3D dataset with the answer [pool table](#). Right is one data from the ScannetV2 dataset with the answer [fireplace](#).

Notably, LISA [24] introduces a specialized segmentation token into its vocabulary, decoded to generate a segmentation mask, enabling more precise and detailed reasoning capabilities.

Recent efforts have extended large language models (LLMs) to include 3D data, thereby improving point cloud understanding. Point-LLM [49] interprets object-level points using LLMs, while 3D-LLM [17] enhances understanding by integrating multi-view image features with LLMs. LL3DA [8] combines textual instructions with visual interactions to improve feature extraction for more effective instruction-following. Unlike existing methods, which are limited to bounding box-level grounding, textual responses, or lack contextual reasoning, our approach enables fine-grained segmentation of precisely searched objects within 3D data.

3 3D Reasoning Segmentation

Problem Definition. 3D reasoning segmentation task involves generating a 3D segmentation map \mathbf{M} from a given 3D scene point cloud \mathbf{P} alongside a complex textual instruction \mathbf{X}_{txt} . This instruction often demands sophisticated linguistic comprehension, extending beyond mere identification tasks, like 3D referring segmentation task [19]. For instance, rather than processing simple directives like "the red chair," the textual queries might involve intricate descriptions or scenarios, such as "an object usually situated in a living room that can accommodate multiple people sitting together comfortably," which requires in-depth world knowledge and reasoning understanding.

Dataset Collection. Given the absence of a standardized dataset for evaluating 3D reasoning segmentation, we have collected the 3D scans from indoor datasets, Matterport3D [6] and ScanNetv2 [13] and annotated them with complex text instructions and detailed 3D segmentation masks. The dataset consists of 1339 samples for training and 1145 samples for validation. Two sample data are shown in Figure 2. More details can be found in the Appendix.

4 Reason3D

We introduce Reason3D, a novel LLM-based framework for searching and reasoning within 3D point clouds, as illustrated in Figure 3. Given a 3D point cloud and a textual query describing an object of interest, our method leverages an LLM model to align point features and predict dense object segmentation masks. Section 4.1 discusses the alignment of point clouds with LLMs in the feature space. Section 4.2 introduces the proposed hierarchical mask decoder that employs a coarse-to-fine approach for generating dense segmentation masks. Section 4.3 then details the training loss of our Reason3D framework.

4.1 Alignment between LLMs and Point Cloud

Given a point cloud $\mathbf{P} \in \mathbb{R}^{N \times 6}$ consisting of N points, each characterized by three colors channels (r, g, b) and three coordinates (x, y, z), we aim to extract point features and align them with existing decoder-only LLM models to facilitate scene understanding for answering complex questions.

Scene Encoder. We employ a voxelization operation on the point cloud and utilize a U-Net style backbone [16] to extract point-wise features $\mathbf{F}_p \in \mathbb{R}^{N \times C}$, where C denotes the channel dimension. To further reduce complexity, we feed these features into a superpoint pooling layer that utilizes pre-computed superpoints [25]. This layer aggregates superpoint features $\mathbf{F}_s \in \mathbb{R}^{M \times C}$ through

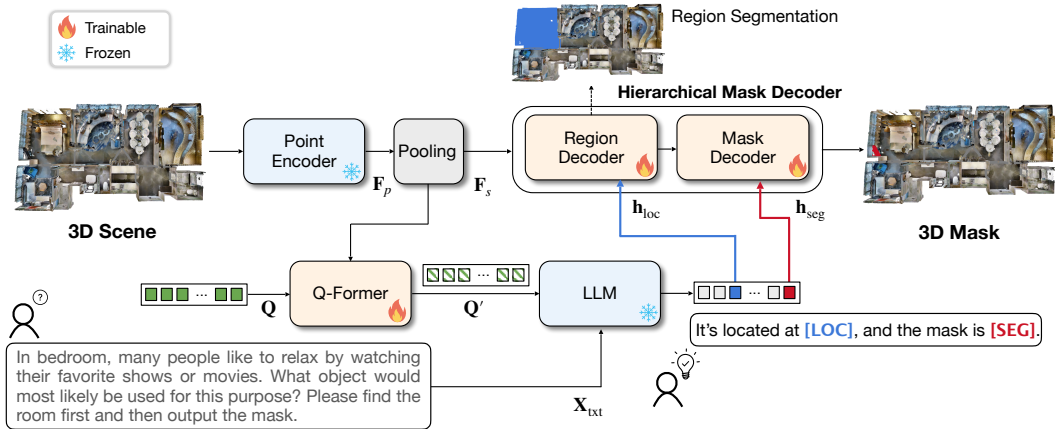


Figure 3: **Overview of our Reason3D framework.** Initially, we utilize a point encoder to extract dense features \mathbf{F}_p from the input scene, simplified by a superpoint pooling layer to reduce complexity. An interactor merges superpoint features \mathbf{F}_s with a learnable query, input into a frozen LLM along with instructions to generate an output containing critical tokens, $[\text{LOC}]$ and $[\text{SEG}]$. A hierarchical decoder then uses the $[\text{LOC}]$ embedding to estimate a coarse location that likely covers the object. Finally, this estimated location integrates with the $[\text{SEG}]$ embedding, enabling the prediction of the final segmentation masks.

average pooling of the point-wise features within each superpoint, effectively reducing the number of points from N to M , where M represents the number of superpoints.

This reduction is crucial for managing large-scale scenes without the need to segment the point cloud into smaller segments. For instance, a single Matterport3D scene [6] contains approximately one million points—a significant challenge for existing algorithms [31] that typically require data segmentation. Our approach significantly reduces complexity and enhances processing efficiency by handling extensive data in a single pass.

Alignment with LLM. To align the superpoint features \mathbf{F}_s with existing decoder-only LLM models, we employ an interactor \mathcal{F} following Q-Former [26] to facilitate dynamic interaction between the point cloud features \mathbf{F}_s and the learnable query \mathbf{Q} , resulting in an updated query $\mathbf{Q}' = \mathcal{F}(\mathbf{Q}, \mathbf{F}_s)$. Subsequently, the updated query \mathbf{Q}' and textual instructions \mathbf{X}_{txt} are fed into a frozen decoder-only language model (LLM) to generate targeted responses:

$$\mathbf{Y}_{\text{txt}} = \text{LLM}(\mathbf{Q}', \mathbf{X}_{\text{txt}}). \quad (1)$$

We freeze the point cloud encoders and the LLM, allowing updates only to the interactor module. This setup focuses on learning interactions between 3D and linguistic data, enhancing the model’s ability to produce accurate, contextually relevant responses to textual commands about 3D data.

4.2 Hierarchical Mask Decoder

Existing 3D scene-level LLM-based methods [17, 8] primarily produce textual or numerical outputs and cannot provide predictions for dense 3D masks. To overcome these limitations, we introduce a Hierarchical Mask Decoder that seamlessly integrates with the outputs of LLMs. This advanced integration allows our system to interpret textual instructions and generate corresponding detailed segmentation masks directly.

The Hierarchical Mask Decoder predicts the masks \mathbf{M} , \mathbf{M} , using the superpoint features \mathbf{F}_s of the input scene and prompts $\langle \mathbf{P}_{\text{loc}}, \mathbf{P}_{\text{seg}} \rangle$ generated from the LLM output based on the instruction \mathbf{X}_{txt} :

$$\mathbf{M} = \text{Decoder}(\mathbf{Q}_h; \langle \mathbf{P}_{\text{loc}}, \mathbf{P}_{\text{seg}} \rangle | \langle \mathbf{F}_s, \mathbf{X}_{\text{txt}} \rangle), \quad (2)$$

where \mathbf{Q}_h is a learnable object query and \mathbf{P}_{loc} and \mathbf{P}_{seg} denote the location and segmentation prompts, respectively. Inspired by LISA [24], which directs an LLM to output specific embedding tokens, we adopt a similar strategy. Our LLM is prompted to produce a $[\text{SEG}]$ token. The last-layer

embedding \mathbf{h}_{seg} associated with the [SEG] token is transformed through an MLP projection layer \mathcal{G} , resulting in the segmentation prompt $\mathbf{P}_{seg} = \mathcal{G}(\mathbf{h}_{seg})$, which is derived from the complex textual instructions to guide the final mask prediction.

Moreover, for effective 3D mask prediction, especially when targeting small objects within large scenes. We propose a coarse-to-fine approach. We further introduce a special token, [LOC], to learn the coarse location that may encompass the object mask. Similar to the [SEG] token process, we refine the embedding \mathbf{h}_{loc} of the [LOC] token using an MLP layer \mathcal{G} , resulting in $\mathbf{P}_{loc} = \mathcal{G}(\mathbf{h}_{loc})$. To this end, we can use two prompts to guide the final mask prediction. In practice, we initially exploit a mask decoder, \mathcal{F}_{loc} , constructed with a transformer decoder architecture [37, 38]. Tguidingecoder uses the location prompt as the query to generate a location mask \mathbf{M}_{loc} :

$$\mathbf{M}_{loc} = \mathcal{F}_{loc}(\mathbf{P}_{loc}, \mathbf{F}_s). \quad (3)$$

Subsequently, the location mask \mathbf{M}_{loc} serves as a prior to guide the final mask generation through another MLP layer \mathcal{H}_{loc} :

$$\mathbf{M} = \mathcal{F}_{seg}(\mathbf{P}_{seg}, \mathbf{F}_s + \mathcal{H}_{loc}(\mathbf{M}_{loc})), \quad (4)$$

where \mathbf{M} is the final mask, and \mathcal{F}_{seg} shares the same architectural framework as \mathcal{F}_{loc} .

4.3 Training 3D LLM

The loss function for Reason3D comprises two essential components: the LLM loss \mathcal{L}_{llm} and the segmentation mask loss \mathcal{L}_{mask} . The overall combination is represented as:

$$\mathcal{L} = \mathcal{L}_{llm} + \mathcal{L}_{mask}. \quad (5)$$

In particular, The LLM loss, \mathcal{L}_{llm} , embodies the linguistic aspects through an auto-regressive cross-entropy loss for text generation, incorporating cross-entropy loss CE for each token:

$$\mathcal{L}_{llm} = \text{CE}(\mathbf{Y}_{txt}, \hat{\mathbf{Y}}_{txt}) \quad (6)$$

where $\hat{\mathbf{Y}}_{txt}$ represents the ground truth word token. In addition, the mask loss \mathcal{L}_{mask} aims at encouraging the model to generate high-quality segmentation masks. This loss is computed using a binary cross-entropy (BCE) loss and DICE loss for all superpoints, which is represented as:

$$\mathcal{L}_{mask_*} = \text{BCE}(\mathbf{M}_*, \hat{\mathbf{M}}_*) + \text{DICE}(\mathbf{M}_*, \hat{\mathbf{M}}_*), * \in [loc, seg]. \quad (7)$$

where $\hat{\mathbf{M}}_*$ means the ground truth segmentation mask for region-level and object-level superpoints. For the object-level mask $\hat{\mathbf{M}}_{seg}$, we utilize the mask of the object that we target. For the region-level mask $\hat{\mathbf{M}}_{loc}$, we mark the points as the foreground points if the distance between any point and the object center is smaller than threshold τ .

5 Experiments

5.1 Experimental Setting

Datasets. Our training data includes three main types of datasets: (1) For the 3D expressive referring segmentation task, we use ScanRefer [7] and Sr3D datasets [1]. (2) For the 3D question answering task, we utilize ScanQA dataset [4]. (3) For the 3D reasoning segmentation task, we use the Reason3D datasets, which we annotated from both the ScanNetV2 and Matterport3D datasets. The results of 3D QA and more details are included in the Appendix.

Model Architecture. We use a pre-trained Sparse 3D U-Net [38] to extract point-wise features. For the language learning model, we employ FlanT5 [12], maintaining most of its pre-trained weights frozen, except for adapting the weights for the newly-added location and segmentation tokens. Our QFormer is constructed by the BLIP-2 [26] architecture, incorporating 1408-dimensional features.

Evaluation Metrics. For the 3D expressive referring segmentation and 3D reasoning segmentation tasks, the primary evaluation metrics are Mean Intersection over Union (mIoU), which quantifies the average overlap between the predicted and true 3D volumes, and Accuracy at k Intersection over Union (Acc@kIoU). This latter metric measures the proportion of descriptions for which the predicted mask overlaps the ground truth with an IoU greater than k, where k is set at thresholds of 0.25 and 0.5, thus assessing the model’s performance at varying levels of precision. For the QA task, the evaluation metrics include BLEU-4 [30], ROUGE-L [27], METEOR [5], and CIDEr [43] to ensure robust answer matching. These metrics evaluate the precision, fluency, and semantic accuracy of the responses.

Method	Venue	ScanNet			Matterport3D		
		0.25	0.50	mIoU	0.25	0.50	mIoU
OpenScene [31]	CVPR'23	4.22	0.97	5.03	4.07	0.57	6.36
OpenScene [31]+FlanT5 [12]	CVPR'23+ArXiv'22	24.68	7.14	15.03	19.98	4.02	13.60
OpenMask3D [39]	NeurIPS'23	5.70	3.25	7.14	3.25	0.12	5.96
OpenMask3D [39]+FlanT5 [12]	NeurIPS'23+ArXiv'22	20.78	6.82	13.38	17.46	0.23	9.07
3D-STMN [45]	AAAI'24	25.43	17.78	18.23	20.68	10.81	13.47
Llama2 [20]+CLIP [35]	ArXiv'23+ArXiv'22	39.26	25.93	27.23	28.51	14.86	17.80
Reason3D (Ours)	-	43.21	32.10	31.20	31.22	17.43	19.54

Table 1: **3D Reasoning Segmentation Results** on Reason3D dataset. The evaluation metric is accuracy at IoU 0.25, IoU 0.5 and mIoU.

Method	Venue	Unique (~19%)			Multiple (~81%)			Overall		
		0.25	0.50	mIoU	0.25	0.50	mIoU	0.25	0.50	mIoU
ScanRefer [7]*	ECCV'20	67.6	44.4	39.9	31.2	20.9	19.5	38.2	25.5	23.5
3DVG-Transformer [56]*	ICCV'21	79.5	58.0	49.9	42.0	30.8	27.0	49.3	36.1	31.4
3D-SPS [29]*	CVPR'22	84.8	65.6	54.7	41.7	30.8	26.7	50.1	37.6	32.1
3D-LLM [17]*	NeurIPS'23	57.8	30.6	32.5	24.7	12.8	14.0	31.1	16.3	17.6
TGNM [19]	AAAI'21	69.3	57.8	50.7	31.2	26.6	23.6	38.6	32.7	28.8
X-RefSeg3D [34]	AAAI'24	-	-	-	-	-	-	40.3	33.8	29.9
3D-STMN [45]	AAAI'24	89.3	84.0	74.5	46.2	29.2	31.1	54.6	39.8	39.5
Reason3D (Ours)	-	88.4	84.2	74.6	50.5	31.7	34.1	57.9	41.9	42.0

Table 2: **3D Referring Expression Segmentation Results** on ScanRefer dataset with the accuracy evaluated by IoU 0.25, IoU 0.5 and mIoU. For the first block methods * that only output 3D bounding boxes, we reproduce the results based on their official codes by extracting the points inside the boxes as the segmentation mask predictions.

5.2 3D Reasoning Segmentation Results

We present the results of our 3D reasoning segmentation in Table 1. Our model significantly surpasses previous models in tasks that require advanced reasoning and a deep understanding of world knowledge, achieving a notable increase in mean Intersection over Union (mIoU). Differing from typical 3D referring segmentation tasks, this task demands not just an understanding of spatial relationships but also robust reasoning capabilities and a broad comprehension of context.

Our model excels at interpreting long sentence queries and managing 3D reasoning segmentation tasks, outperforming open-vocabulary segmentation methods such as OpenScene [31] and OpenMask3D [39]. We also compare its performance against a two-stage method, where FlanT5 generates a short text output for the query in the first stage, followed by segmentation using either OpenScene or OpenMask3D. Our method surpasses this approach by leveraging more expressive hidden embeddings, which provide a richer representation than solely relying on text as an intermediary.

Compared with leading 3D referring segmentation models, specifically 3D-STMN [45] fine-tuned on the Reason3D dataset, we observe that although 3D-STMN excels in direct referencing, it struggles with indirect queries. In contrast, our model adeptly navigates these challenges by integrating large language models, thereby demonstrating superior adaptability and performance.

In addition, we compare our model to another two-stage method that combines Llama2 [20] and CLIP [35], both fine-tuned on the Reason3D dataset. This approach begins with Llama2 generating an output vocabulary, which CLIP then processes to extract textual features. These features act as queries interacting with point cloud features via a mask decoder (we exploit the same point features and mask decoder as our method), ultimately producing the segmentation mask results. The results demonstrate that our approach significantly outperforms this two-stage method, which is completely decoupled and relies solely on the textual outputs from the LLM model.

Method	Room Num = 1~2			Room Num = 3~4			Room Num >= 5		
	0.25	0.50	mIoU	0.25	0.50	mIoU	0.25	0.50	mIoU
Reason3D (w/o HMD)	25.23	10.32	15.56	12.84	5.50	8.23	8.26	2.52	5.33
Region Seg + Reason3D (w/o HMD)	26.98	13.21	17.02	19.21	8.21	11.67	11.96	4.78	7.21
Reason3D (w/ HMD)	29.82	16.97	18.81	22.25	11.93	14.12	16.06	7.34	10.35

Table 3: **3D Reasoning Segmentation Results** on Matterport3D dataset with different room numbers to validate the effectiveness of the design of the proposed Hierarchical Mask Decoder (HMD). The evaluation metric is IoU@0.25, IoU@0.5 and mIoU.

5.3 3D Referring Expression Segmentation Results

To demonstrate the effectiveness of our model in the 3D express referring segmentation task, we compare our approach against current state-of-the-art methods on ScanRefer validation set in Table 2. It can be observed that our approach significantly outperforms 3D-STMN [45] in overall performance. Considering the limited focus on the 3D referring segmentation task in the existing literature, we extend our comparison to several 3D grounding approaches that only predict 3D bounding boxes. These methods can predict segmentation masks by simply extracting points within the predicted boxes. Notably, our approach vastly outperforms the LLM-based method, 3D-LLM [17], which struggles with accurately locating 3D boxes and effectively extracting segmentation masks.

5.4 Ablation Study

Effectiveness of Hierarchical Mask Decoder. We present experimental results in Table 3 to demonstrate the effectiveness of our proposed Hierarchical Mask Decoder (HMD) design in searching objects across varying numbers of rooms. Since the Reason3D dataset primarily focuses on single-room scenarios, we extend it to multi-room settings by reusing a subset of the annotated Matterport3D [6] data to include a varying number of regions. We opt not to utilize ScanNet, as it features only single-room scenes.

We establish three variants of our Reason3D model: (1) Reason3D without the Hierarchical Mask Decoder, (2) Reason3D combined with a region segmentation module that first predicts and segment the target room’s region then applying the Reason3D model for the segmented region, and (3) Reason3D equipped with the Hierarchical Mask Decoder. We can validate the effectiveness of the proposed Hierarchical Mask Decoder (HMD) by comparing the first and last models, especially when the number of rooms exceeds five. The effectiveness of the HMD is likely due to the difficulty of integrating language embeddings with point cloud features as the number of points increases (*i.e.*, in more rooms scenarios). In contrast, the hierarchical strategy of the HMD, which uses an additional token to learn a coarse region as a prior, effectively manages the output segmentation masks. In addition, the second model segments point clouds from the region of interest before using the Reason3D framework without the HMD. This method outperforms the first model but faces optimization challenges within the training pipeline of the two-stage approach.

Effectiveness of Different Designs. Table 4 shows the ablation experiments of different choices. Table 4(a) proves that the superpoints pooling operation is essential for our pipeline since it helps to reduce the training complexity and enables the effective training of the pipeline. Also, the average pooling for the superpoints can achieve better performance. Table 4(b) presents the performance impact of various components of segmentation loss. Using either Binary Cross-Entropy (BCE) loss or Dice loss alone leads to significantly reduced performance. In contrast, combining Dice loss and

Superpoint	Pool	Acc@0.25	Time (ms)	DICE	BCE	Acc@0.25	Acc@0.50	Layer	Acc@0.25	Acc@0.50
✗	-	37.55	486.1	✓		41.73	31.36	1	40.25	27.65
✓	max	42.97	271.3	✓	✓	30.86	22.47	3	42.78	30.62
✓	Avg	43.21	268.5	✓	✓	43.21	32.10	6	43.21	32.10

(a) Superpoint Pooling.

(b) Segmentation Loss.

(c) Layer of Decoders.

Table 4: **Ablation experiments** for different design on the scannetV2 dataset for the 3D reasoning segmentation task.

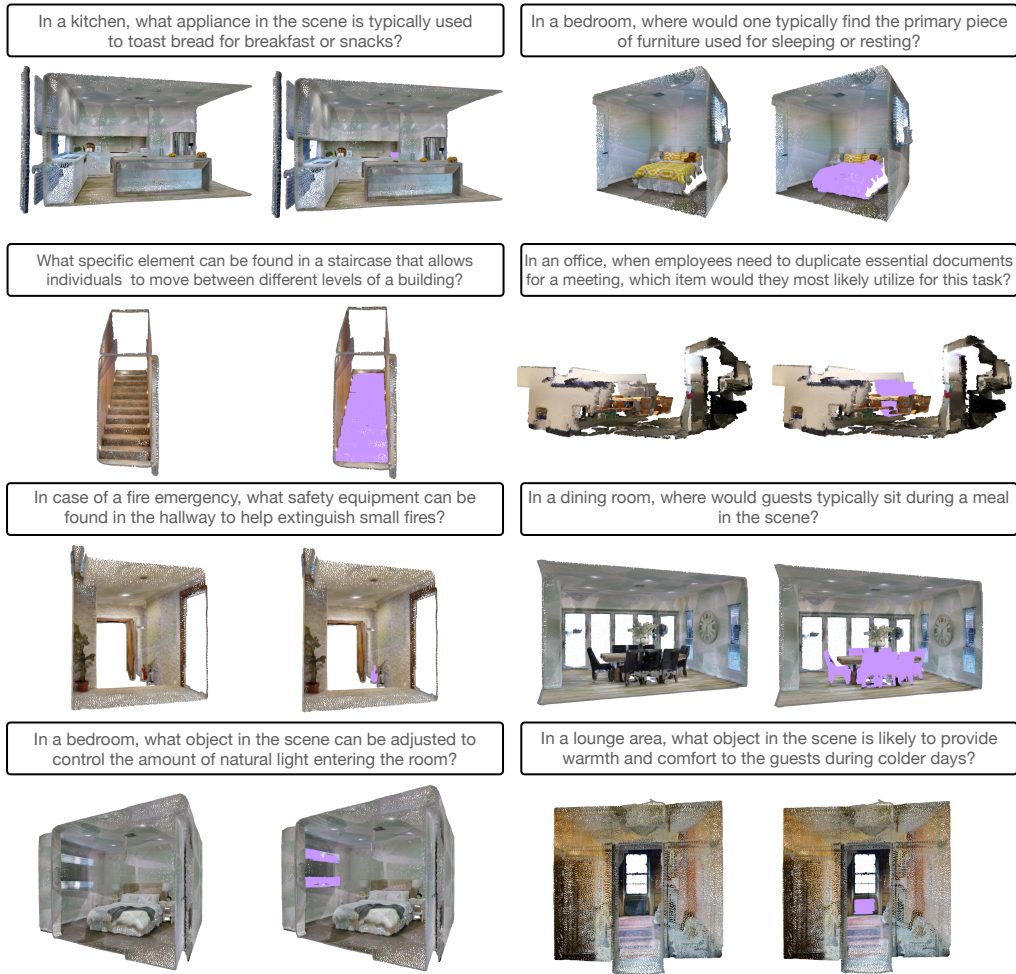


Figure 4: **Visualization Results for 3D Reasoning Segmentation Tasks.** Each sub-figure presents a textual query alongside the input point cloud. The purple regions highlight the predicted segmentation masks generated by our model.

BCE loss results in the most favorable outcomes. Table 4(c) presents the impact of different numbers of decoder layers. We use 6 layers for the decoder as the default number.

5.5 Visualization Results

Figure 4 displays the visualization results of our Reason3D model for the 3D reasoning segmentation task, highlighting our model’s proficiency in accurately generating segmentation masks based on the query. Additional visualization results are included in the Appendix.

6 Conclusion

This study presents Reason3D, an innovative framework that leverages Large Language Models (LLMs) for enhanced scene understanding, capable of generating textual responses and segmentation predictions. To demonstrate the effectiveness of our approach, we introduce the novel task of 3D reasoning segmentation, which requires interpreting implicit human instructions within three-dimensional scenes. We have developed a hierarchical mask decoder that improves the accuracy of final mask predictions by initially identifying a broad region likely to contain the target object, which then serves as a basis for further refinement. Our extensive experiments on the ScanNetV2 and Matterport3D datasets demonstrate outstanding performance in various complex tasks, including 3D reasoning segmentation, 3D referring segmentation, and question answering.

References

- [1] Panos Achlioptas, Ahmed Abdelreheem, Fei Xia, Mohamed Elhoseiny, and Leonidas Guibas. Referit3d: Neural listeners for fine-grained 3d object identification in real-world scenes. In *ECCV*, 2020. 3, 6, 14
- [2] Jean-Baptiste Alayrac, Jeff Donahue, Pauline Luc, Antoine Miech, Iain Barr, Yana Hasson, Karel Lenc, Arthur Mensch, Katie Millican, Malcolm Reynolds, Roman Ring, Eliza Rutherford, Serkan Cabi, Tengda Han, Zhitao Gong, Sina Samangooei, Marianne Monteiro, Jacob Menick, Sebastian Borgeaud, Andy Brock, Aida Nematzadeh, Sahand Sharifzadeh, Mikolaj Binkowski, Ricardo Barreira, Oriol Vinyals, Andrew Zisserman, and Karen Simonyan. Flamingo: a visual language model for few-shot learning. In *NeurIPS*, 2022. 3
- [3] Anas Awadalla, Irena Gao, Josh Gardner, Jack Hessel, Yusuf Hanafy, Wanrong Zhu, Kalyani Marathe, Yonatan Bitton, Samir Gadre, Shiori Sagawa, Jenia Jitsev, Simon Kornblith, Pang Wei Koh, Gabriel Ilharco, Mitchell Wortsman, and Ludwig Schmidt. Openflamingo: An open-source framework for training large autoregressive vision-language models. *arXiv preprint arXiv:2308.01390*, 2023. 1, 3
- [4] Daichi Azuma, Taiki Miyanishi, Shuhei Kurita, and Motoaki Kawanabe. Scanqa: 3d question answering for spatial scene understanding. In *CVPR*, 2022. 6, 14, 15
- [5] Satanjeev Banerjee and Alon Lavie. METEOR: An automatic metric for MT evaluation with improved correlation with human judgments. In *ACL Workshop*, 2005. 6
- [6] Angel Chang, Angela Dai, Thomas Funkhouser, Maciej Halber, Matthias Niessner, Manolis Savva, Shuran Song, Andy Zeng, and Yinda Zhang. Matterport3D: Learning from RGB-D data in indoor environments. In *3DV*, 2017. 3, 4, 5, 8, 13, 14
- [7] Dave Zhenyu Chen, Angel X Chang, and Matthias Nießner. Scanrefer: 3d object localization in rgb-d scans using natural language. In *ECCV*, 2020. 3, 6, 7, 14, 15
- [8] Sijin Chen, Xin Chen, Chi Zhang, Mingsheng Li, Gang Yu, Hao Fei, Hongyuan Zhu, Jiayuan Fan, and Tao Chen. Ll3da: Visual interactive instruction tuning for omni-3d understanding, reasoning, and planning. In *CVPR*, 2024. 1, 4, 5
- [9] Shaoyu Chen, Jiemin Fang, Qian Zhang, Wenyu Liu, and Xinggang Wang. Hierarchical aggregation for 3d instance segmentation. In *ICCV*, 2021. 3
- [10] Shizhe Chen, Makarand Tapaswi, Pierre-Louis Guhur, Cordelia Schmid, and Ivan Laptev. Language conditioned spatial relation reasoning for 3d object grounding. In *NeurIPS*, 2022. 15
- [11] Christopher Choy, JunYoung Gwak, and Silvio Savarese. 4d spatio-temporal convnets: Minkowski convolutional neural networks. In *CVPR*, 2019. 3
- [12] Hyung Won Chung, Le Hou, Shayne Longpre, Barret Zoph, Yi Tay, William Fedus, Eric Li, Xuezhi Wang, Mostafa Dehghani, Siddhartha Brahma, and et al. Scaling instruction-finetuned language models. *arXiv preprint arXiv:2210.11416*, 2022. 6, 7
- [13] Angela Dai, Angel X. Chang, Manolis Savva, Maciej Halber, Thomas Funkhouser, and Matthias Nießner. Scannet: Richly-annotated 3d reconstructions of indoor scenes. In *CVPR*, 2017. 3, 4, 13
- [14] Wenliang Dai, Junnan Li, Dongxu Li, Anthony Meng Huat Tiong, Junqi Zhao, Weisheng Wang, Boyang Li, Pascale Fung, and Steven Hoi. Instructblip: Towards general-purpose vision-language models with instruction tuning. *arXiv preprint arXiv:2305.06500*, 2023. 1, 3
- [15] Martin Ester, Hans-Peter Kriegel, Jörg Sander, and Xiaowei Xu. A density-based algorithm for discovering clusters in large spatial databases with noise. In *KDD*, 1996. 14
- [16] Benjamin Graham, Martin Engelcke, and Laurens van der Maaten. 3d semantic segmentation with submanifold sparse convolutional networks. In *CVPR*, 2018. 4
- [17] Yining Hong, Haoyu Zhen, Peihao Chen, Shuhong Zheng, Yilun Du, Zhenfang Chen, and Chuang Gan. 3d-llm: Injecting the 3d world into large language models. In *NeurIPS*, 2023. 1, 4, 5, 7, 8, 14, 15
- [18] Ji Hou, Angela Dai, and Matthias Nießner. 3d-sis: 3d semantic instance segmentation of rgb-d scans. In *CVPR*, 2019. 3
- [19] Pin-Hao Huang, Han-Hung Lee, Hwann-Tzong Chen, and Tyng-Luh Liu. Text-guided graph neural networks for referring 3d instance segmentation. In *AAAI*, 2021. 3, 4, 7, 15
- [20] Louis Martin Hugo Touvron, Kevin Stone, Peter Albert, Amjad Almahairi, Yasmine Babaei, Nikolay Bashlykov, Soumya Batra, Prajjwal Bhargava, Shruti Bhosale, and et al. Llama 2: Open foundation and fine-tuned chat models. *arXiv:2307.09288*, 2023. 1, 3, 7
- [21] Srinivasan Iyer, Xi Victoria Lin, Ramakanth Pasunuru, Todor Mihaylov, Daniel Simig, Ping Yu, Kurt Shuster, Tianlu Wang, Qing Liu, Punit Singh Koura, Xian Li, Brian O’Horo, Gabriel Pereyra, Jeff Wang, Christopher Dewan, Asli Celikyilmaz, Luke Zettlemoyer, and Ves Stoyanov. Opt-impl: Scaling language model instruction meta learning through the lens of generalization. *arXiv preprint arXiv:2212.12017*, 2022. 3
- [22] Zhao Jin, Munawar Hayat, Yuwei Yang, Yulan Guo, and Yinjie Lei. Context-aware alignment and mutual masking for 3d-language pre-training. In *CVPR*, 2023. 15
- [23] Maxim Kolodiazhnyi, Anna Vorontsova, Anton Konushin, and Danila Rukhovich. Oneformer3d: One transformer for unified point cloud segmentation. *arXiv preprint arXiv:2311.14405*, 2023. 3

- [24] Xin Lai, Zhuotao Tian, Yukang Chen, Yanwei Li, Yuhui Yuan, Shu Liu, and Jiaya Jia. Lisa: Reasoning segmentation via large language model. In *CVPR*, 2024. 2, 3, 4, 5
- [25] Loic Landrieu and Martin Simonovski. Large-scale point cloud semantic segmentation with superpoint graphs. In *CVPR*, 2018. 4
- [26] Junnan Li, Dongxu Li, Silvio Savarese, and Steven Hoi. Blip-2: Bootstrapping language-image pre-training with frozen image encoders and large language models. *arXiv preprint arXiv:2301.12597*, 2023. 1, 3, 5, 6
- [27] Chin-Yew Lin. Rouge: A package for automatic evaluation of summaries. In *Text summarization branches out*, 2004. 6
- [28] Haotian Liu, Chunyuan Li, Qingyang Wu, and Yong Jae Lee. Visual instruction tuning. In *NeurIPS*, 2023. 1, 3
- [29] Junyu Luo, Jiahui Fu, Xianghao Kong, Chen Gao, Haibing Ren, Hao Shen, Huaxia Xia, and Si Liu. 3d-sps: Single-stage 3d visual grounding via referred point progressive selection. *arXiv preprint arXiv:2204.06272*, 2022. 7, 15
- [30] Kishore Papineni, Salim Roukos, Todd Ward, and Wei-Jing Zhu. Bleu: a method for automatic evaluation of machine translation. In *ACL*, 2002. 6
- [31] Songyou Peng, Kyle Genova, Chiyu "Max" Jiang, Andrea Tagliasacchi, Marc Pollefeys, and Thomas Funkhouser. Openscene: 3d scene understanding with open vocabularies. In *CVPR*, 2023. 3, 5, 7
- [32] Zekun Qi, Runpei Dong, Shaochen Zhang, Haoran Geng, Chunrui Han, Zheng Ge, He Wang, Li Yi, and Kaisheng Ma. Shapellm: Universal 3d object understanding for embodied interaction. *arXiv preprint arXiv:2402.17766*, 2024. 1
- [33] Zhangyang Qi, Ye Fang, Zeyi Sun, Xiaoyang Wu, Tong Wu, Jiaqi Wang, Dahua Lin, and Hengshuang Zhao. Gpt4point: A unified framework for point-language understanding and generation. In *CVPR*, 2024. 1
- [34] Zhipeng Qian, Yiwei Ma, Jiayi Ji, and Xiaoshuai Sun. X-refseg3d: Enhancing referring 3d instance segmentation via structured cross-modal graph neural networks. In *AAAI*, 2024. 3, 7
- [35] Alec Radford, Jong Wook Kim, Chris Hallacy, Aditya Ramesh, Gabriel Goh, Sandhini Agarwal, Girish Sastry, Amanda Askell, Pamela Mishkin, Jack Clark, Gretchen Krueger, and Ilya Sutskever. Learning transferable visual models from natural language supervision. *arXiv preprint arXiv:2103.00020*, 2021. 7
- [36] Hanoona Rasheed, Muhammad Maaz, Sahal Shaji, Abdelrahman Shaker, Salman Khan, Hisham Cholakkal, Rao M. Anwer, Eric Xing, Ming-Hsuan Yang, and Fahad S. Khan. Glamm: Pixel grounding large multimodal model. In *CVPR*, 2024. 1
- [37] Jonas Schult, Francis Engelmann, Alexander Hermans, Or Litany, Siyu Tang, and Bastian Leibe. Mask3D: Mask Transformer for 3D Semantic Instance Segmentation. In *ICRA*, 2023. 3, 6
- [38] Jiahao Sun, Chunmei Qing, Junpeng Tan, and Xiangmin Xu. Superpoint transformer for 3d scene instance segmentation. *arXiv preprint arXiv:2211.15766*, 2022. 3, 6, 13
- [39] Ayça Takmaz, Elisabetta Fedele, Robert W. Sumner, Marc Pollefeys, Federico Tombari, and Francis Engelmann. OpenMask3D: Open-Vocabulary 3D Instance Segmentation. In *NeurIPS*, 2023. 7
- [40] Yuan Tang, Xu Han, Xianzhi Li, Qiao Yu, Yixue Hao, Long Hu, and Min Chen. Minigt-3d: Efficiently aligning 3d point clouds with large language models using 2d priors. *arXiv preprint arXiv:2405.01413*, 2024. 1
- [41] OpenAI teams. Gpt-4 technical report. *arXiv preprint arXiv:2303.08774*, 2023. 1, 3
- [42] Hugo Touvron, Thibaut Lavril, Gautier Izacard, Xavier Martinet, Marie-Anne Lachaux, Timothée Lacroix, Baptiste Rozière, Naman Goyal, Eric Hambro, Faisal Azhar, Aurelien Rodriguez, Armand Joulin, Edouard Grave, and Guillaume Lample. Llama: Open and efficient foundation language models. *arXiv:2302.13971*, 2023. 1, 3
- [43] Ramakrishna Vedantam, C Lawrence Zitnick, and Devi Parikh. Cider: Consensus-based image description evaluation. In *CVPR*, 2015. 6
- [44] Peng-Shuai Wang. Octformer: Octree-based transformers for 3D point clouds. In *SIGGRAPH*, 2023. 3
- [45] Changli Wu, Yiwei Ma, Qi Chen, Haowei Wang, Gen Luo, Jiayi Ji, and Xiaoshuai Sun. 3d-stmn: Dependency-driven superpoint-text matching network for end-to-end 3d referring expression segmentation. In *AAAI*, 2024. 3, 7, 8, 15
- [46] Penghao Wu and Saining Xie. V*: Guided visual search as a core mechanism in multimodal llms. *arXiv preprint arXiv:2312.14135*, 2023. 3
- [47] Tsung-Han Wu, Giscard Biamby, David Chan, Lisa Dunlap, Ritwik Gupta, Xudong Wang, Joseph E. Gonzalez, and Trevor Darrell. See, say, and segment: Teaching llms to overcome false premises. *arXiv preprint arXiv:2312.08366*, 2023. 3
- [48] Xiaoyang Wu, Yixing Lao, Li Jiang, Xihui Liu, and Hengshuang Zhao. Point transformer v2: Grouped vector attention and partition-based pooling. In *NeurIPS*, 2022. 3
- [49] Runsen Xu, Xiaolong Wang, Tai Wang, Yilun Chen, Jiangmiao Pang, and Dahua Lin. Pointllm: Empowering large language models to understand point clouds. *arXiv preprint arXiv:2308.16911*, 2023. 1, 4

- [50] Qinghao Ye, Haiyang Xu, Guohai Xu, Jiabo Ye, Ming Yan, Yiyang Zhou, Junyang Wang, Anwen Hu, Pengcheng Shi, Yaya Shi, Chenliang Li, Yuanhong Xu, Hehong Chen, Junfeng Tian, Qi Qian, Ji Zhang, Fei Huang, and Jingren Zhou. mplug-owl: Modularization empowers large language models with multimodality. *arXiv preprint arXiv:2304.14178*, 2023. 1, 3
- [51] Zhihao Yuan, Xu Yan, Yinghong Liao, Ruimao Zhang, Zhen Li, and Shuguang Cui. Instancerefer: Cooperative holistic understanding for visual grounding on point clouds through instance multi-level contextual referring. In *ICCV*, 2021. 15
- [52] Jun Zhan, Junqi Dai, Jiasheng Ye, Yunhua Zhou, Dong Zhang, Zhigeng Liu, Xin Zhang, Ruibin Yuan, Ge Zhang, Linyang Li, et al. Anygpt: Unified multimodal llm with discrete sequence modeling. *arXiv preprint arXiv:2402.12226*, 2024. 1
- [53] Shilong Zhang, Peize Sun, Shoufa Chen, Min Xiao, Wenqi Shao, Wenwei Zhang, Kai Chen, and Ping Luo. Gpt4roi: Instruction tuning large language model on region-of-interest. *arXiv preprint arXiv:2307.03601*, 2023. 3
- [54] Zhuosheng Zhang, Aston Zhang, Mu Li, Hai Zhao, George Karypis, and Alex Smola. Multimodal chain-of-thought reasoning in language models. *arXiv preprint arXiv:2302.00923*, 2023. 1
- [55] Hengshuang Zhao, Li Jiang, Jiaya Jia, Philip HS Torr, and Vladlen Koltun. Point transformer. In *ICCV*, 2021. 3
- [56] Lichen Zhao, Daigang Cai, Lu Sheng, and Dong Xu. 3DVG-Transformer: Relation modeling for visual grounding on point clouds. In *ICCV*, 2021. 7
- [57] Lianmin Zheng, Wei-Lin Chiang, Ying Sheng, Siyuan Zhuang, Zhanghao Wu, Yonghao Zhuang, Zi Lin, Zhuohan Li, Dacheng Li, Eric. P Xing, Hao Zhang, Joseph E. Gonzalez, and Ion Stoica. Judging llm-as-a-judge with mt-bench and chatbot arena. *arXiv preprint arXiv:2306.05685*, 2023. 3
- [58] Deyao Zhu, Jun Chen, Xiaoqian Shen, Xiang Li, and Mohamed Elhoseiny. Minigpt-4: Enhancing vision-language understanding with advanced large language models. *arXiv preprint arXiv:2304.10592*, 2023. 3

Appendix

A Reason3D Dataset

A.1 Dataset annotation

Each 3D scene in the Reason3D dataset consists of a textual query and a binary segmentation mask to identify the target objects. As mentioned in the paper, we utilize ScanNetV2 [13] and Matterport3D [6] as our data source. Considering single room space as one scene, we first extract the instance object annotation and the room type information from these two datasets as the tag of 3D scenes. After that, we utilize these tags as parts of the text prompt to incorporate with GPT-4. The illustration of the prompt construction process is shown in Table 5, and some samples utilized for prompting are shown in Table 6.

```
messages = [{"role": "system", "content": "You are an AI visual assistant, and you are seeing a 3D scene. What you see is provided with several words to represent objects with tag <objects>, describing the scene you are looking at, and also the room type <type> to describe the type of the scene. Design a question <question> that can be answered confidently with the <answer> from one of the provided objects in <objects>. Please do not ask any <question> that cannot be answered confidently. Each question should have one clear answer that is most relevant, without ambiguity or multiple possible answers in the list of description words. Please include complex questions relevant to the scene's content, such as inquiries into the background knowledge of objects or discussions about events related to these objects. Avoid questions about uncertain or unclear details. The question should be natural."}]
for sample in few_shot_samples:
    messages.append({"role": "user", "content": sample['context']})
    messages.append({"role": "assistant", "content": sample['response']})
messages.append({"role": "user", "content": '\n'.join(query)})
```

Table 5: The illustration of the prompt construction process for generating 3D reasoning dataset with ChatGPT / GPT-4.

A.2 Dataset Statistics

As detailed in the main paper, the Reason3D dataset incorporates the ScanNetV2 and Matterport3D datasets. We adhere to their official training and validation splits for data annotation. Specifically, the Matterport3D dataset provides 934 training samples and 837 validation samples. Meanwhile, the ScanNetV2 dataset contributes 405 training samples and 308 validation samples.

B Experiments

B.1 Implementation Details

We execute the models on two NVIDIA Tesla A100 GPUs, using a batch size of 32 for training and a batch size of 1 for inference. We employ the AdamW optimizer with parameters $\beta_1 = 0.9$ and $\beta_2 = 0.999$, and a weight decay of 0.05. Additionally, we apply a linear warm-up strategy to the learning rate during the initial 1,000 steps, increasing it from 10^{-8} to 10^{-4} , followed by the cosine decay schedule. All experiments are implemented with the Pytorch framework.

B.2 Data Statistics

In addition to the reason3D dataset, our model utilizes the following datasets for training:

ScanNet [13], a comprehensive 3D indoor dataset, covers diverse environments including apartments and various room types. The dataset is structured into 1201 training scenes, 312 validation scenes, and 100 testing scenes. We adopt the training configuration as SPFormer [38] for training our

<p>'context': <room> game room <objects> 'armchair', 'ceiling', 'door', 'doorframe', 'fireplace', 'floor', 'pool table', 'post', 'rail', 'stair', 'stool', 'tv', 'wall', 'window'</p> <p>'response': <question> In a game room, what object in the scene could be used for playing a competitive and strategic game involving balls and cues? <answer> pool table</p>
<p>'context': <room> living room <objects> 'armchair', 'bedroom', 'bookshelf', 'lamp', 'bureau', 'carpet', 'ceiling fan', 'chair', 'computer', 'computer desk', 'couch', 'table', 'drawer', 'dresser'</p> <p>'response': <question> It's very hot outside. After coming back home, what appliance would you turn on to help cool down the temperature? <answer> ceiling fan</p>
<p>'context': <room> game room <objects> 'table', 'door', 'cabinet', 'desk', 'office chair', 'picture', 'lamp', 'bathtub', 'bag', 'trash can', 'mirror', 'radiator'</p> <p>'response': <question> When staying at a hotel, what part of the room in the scene can provide additional lighting for reading or working while in bed? <answer> lamp</p>
<p>'context': <room> game room <objects> 'floor', 'door', 'cabinet', 'shelf', 'desk', 'office chair', 'window', 'monitor', 'book', 'box', 'keyboard', 'trash can', 'file cabinet', 'fan', 'telephone', 'cup', 'paper towel roll', 'windowsill', 'clock', 'headphones'</p> <p>'response': <question> If someone wanted to check the time after getting ready in the morning, what object in this scene would they most likely use? <answer> clock</p>

Table 6: The few shot samples used for ChatGPT prompting.

scene encoder on the ScanNet training dataset.

Matterpor3D [6] dataset is a large-scale, real-world dataset comprising 90 houses. Each house is divided into various regions. We do not fine-tune the scene encoder on the Matterport3D dataset.

ScanRefer [7], a dataset annotated using ScanNet for 3D express referring segmentation tasks, including 36,665 natural language descriptions related to 7,875 objects across 562 scenes for training, and 9,508 descriptions of 2,068 objects from 141 ScanNet scenes for evaluation.

Nr3D [1], another 3D referring segmentation dataset derived from ScanNet, comprises 32,919 language descriptions associated with 4,664 objects from 511 scenes for training purposes. We further employ this dataset to train for 3D express referring segmentation tasks.

ScanQA [4] is a dataset for 3D question answering task based on ScanNet, consisting of 25,563 question-answer pairs on 562 scenes for training and 4,675 question-answer pairs on 71 scenes for validation.

B.3 3D Question Answering Results

In addition to excelling in 3D reasoning and referring tasks, our approach also performs well in 3D question answering tasks. We present our results on the ScanQA validation set in Table 7, where we observed a significant improvement in evaluation metrics over both baseline methods and the recent LLM-based method, 3D-LLM. Our approach not only answers questions accurately but also visualizes the related segmentation masks to further demonstrate the effectiveness.

B.4 3D Visual Grounding Results.

Although our primary focus is on 3D segmentation, our method also effectively predicts 3D bounding boxes as supplementary outputs, facilitating comparison with 3D visual grounding methods. To generate a 3D bounding box for a referred object, we first apply DBSCAN [15] to eliminate noisy points, and then calculate the minimum and maximum XYZ coordinates from the points within the segmentation mask to form the 3D box. As demonstrated in Table 8, our approach not only outperforms recent 3D visual grounding methods but also significantly surpasses LLM-based methods, such as 3D-LLM [17], which struggle to integrate textual and numerical data to accurately localize objects in 3D space.

Method	Venue	B-4	METEOR	ROUHE-L	CIDER
VoteNet+MCAN	-	6.2	11.4	29.8	54.7
ScanRefer+MCAN	-	7.9	11.5	30	55.4
ScanQA [4]	CVPR 2022	10.1	13.1	33.3	64.9
3D-VLP [22]	CVPR 2023	11.2	13.5	34.5	67.0
3D-LLM [17]	NeurIPS 2023	12.0	14.5	35.7	69.4
Reason3D (Ours)	-	12.1	15.1	37.4	73.5

Table 7: **3D question answering results** on ScanQA validation dataset. The first two results are from [4]. B-4 denotes BLEU-4. Our model achieves better results than all baseline models.

Method	Venue	Acc@0.25	Acc@0.50
ScanRefer [7]	ECCV 2020	38.97	26.10
InstanceRefer [51]	ICCV 2021	40.23	32.93
3D-SPS [29]	CVPR 2022	47.65	36.43
ViL3DRel [10]	NeurIPS 2022	47.94	37.73
3D-LLM [17]	NeurIPS 2023	30.3	-
TGNN [19]	AAAI 2021	37.37	29.70
3D-STMN [45]	AAAI 2024	46.8	36.6
Reason3D (Ours)	-	49.60	41.10

Table 8: **3D visual grounding results** on ScanRefer validation dataset. Our approach does not use 3D box annotation for training.

B.5 More Visualization Results.

3D Reasoning Segmentation. We provide more qualitative examples for the 3D reasoning segmentation task and the predictions by our Reason3D in Figure 5.

3D Referring Segmentation. We show the visualization results of the 3D referring segmentation task compared with 3D-STMN [45] in Figure 6. We observe that our approach can have correct predictions when the scenes contain multiple similar objects or when the query sentence is long, which proves the effectiveness of our approach.

C Failure Case.

In Figure 7, we present representative failure cases as follows: (a) If the question involves querying a small object in the scene, our model may fail to generate the correct prediction. (b) The presence of similar objects in the scene may lead to false positive predictions by our model. (c) Similar structures in the point cloud, such as mirrors or sensor-induced fragments, can mislead our model. (d) Complex world knowledge required by the question may hinder our model’s ability to generate accurate mask predictions.

D Limitations

While our model introduces a novel approach to the 3D reasoning segmentation task, it does have several limitations. Firstly, we observe that our model cannot handle very large-scale scenes for 3D reasoning segmentation (*e.g.*, searching for an object within a house with 30 rooms in the Matterport dataset). Furthermore, our model lacks the ability to handle false premises cases (*e.g.*, searching for an object that may not be inside the scenes), which could be a promising direction to explore within the LLM-based 3D reasoning framework.

E Broader Impact

Reason3D is designed to segment objects in 3D space based on language inputs. Compared to traditional 3D segmentation algorithms, Reason3D models have a lower customization threshold, allowing users to identify objects through natural language. However, this accessibility could potentially be abused. Additionally, the datasets and pre-trained models utilized in Reason3D may contain inherent biases, which could be reflected in the model’s performance.

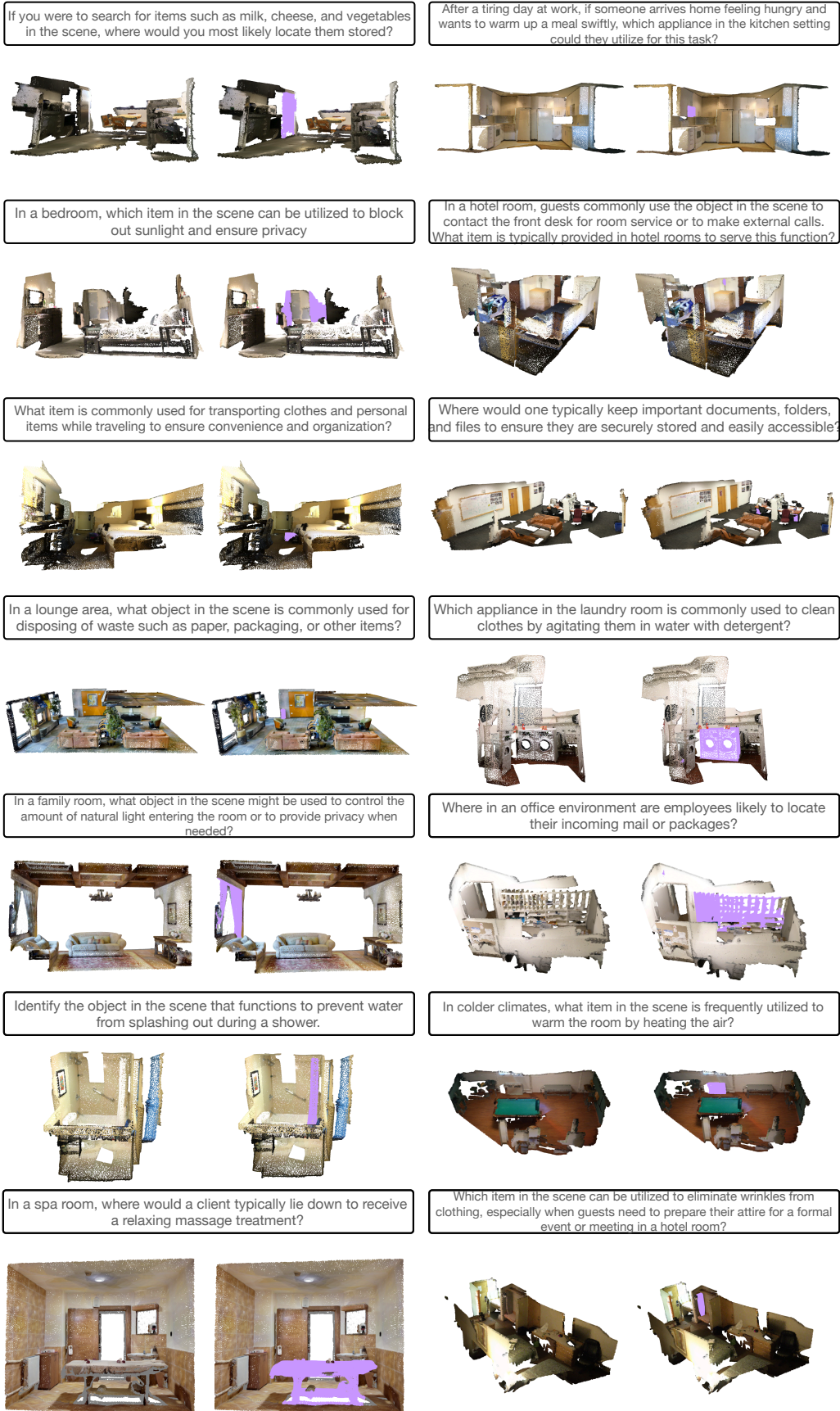


Figure 5: Visualization Results for 3D Reasoning Segmentation Tasks. The purple regions highlight the predicted segmentation masks generated by our model. Best viewed with zoom in.

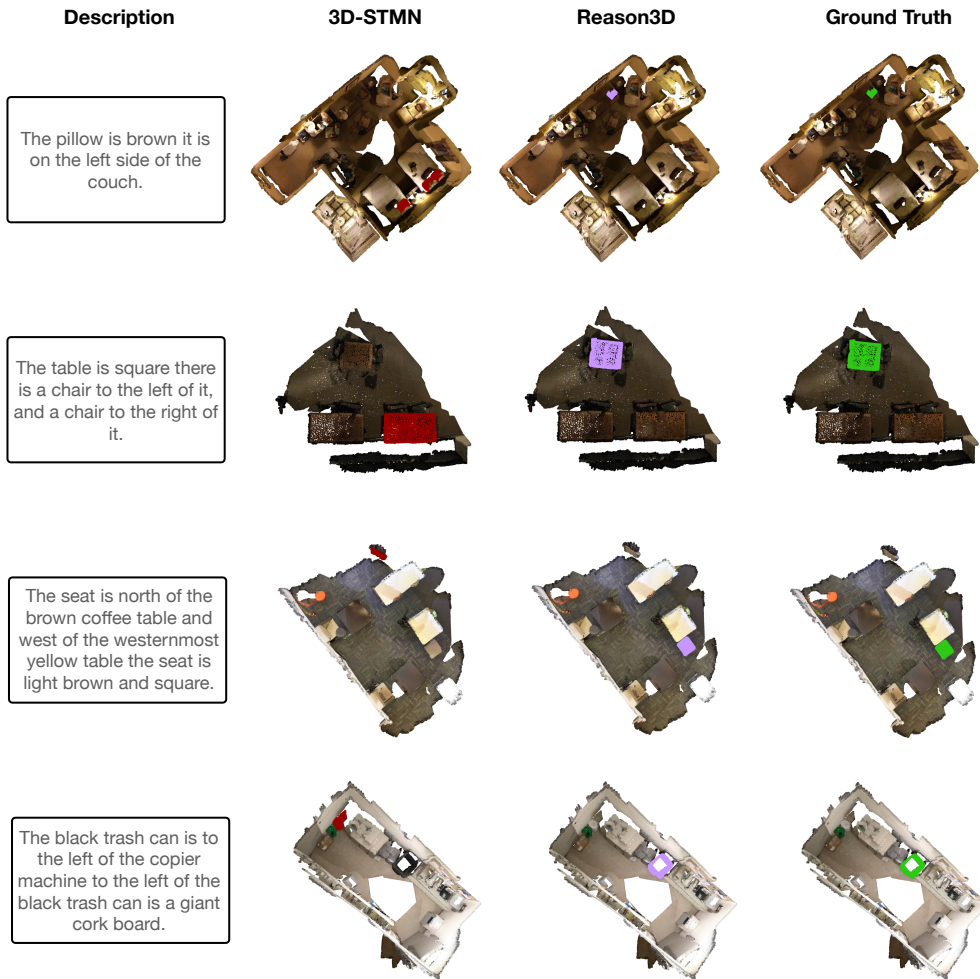


Figure 6: **Visualization Results for 3D Referring Segmentation Tasks.** The purple regions denotes the predicted segmentation masks from our Reason3D. The red and green means the predictions from 3D-STMN and ground truth, respectively. Best viewed with zoom in.

(a.) Small queried object

Safety is crucial in public spaces like spas. What object in the scene is designed to detect and suppress fires to ensure the well-being of everyone in the spa?



(b.) Similar objects in the scene.

In a public restroom, if someone wishes to dry their hands after washing, which item in the scene can they use for this task?



(c.) Similar structures of the point cloud.

What object in the scene would be most useful for checking one's appearance before leaving the bathroom?



(d.) Requiring complicate world knowledge.

In the bathroom, there may be decorative elements on the walls that hold symbolic significance. What object in the scene could be a religious symbol often associated with Christianity?



Figure 7: **Failure cases.** (a.) Small queried objects. (b.) Similar object in the scene. (c.) Similar structures of the point cloud. (d.) The question requiring complicate world knowledge. The purple regions denotes the predicted segmentation masks from our Reason3D and the green means the ground truth. Best viewed with zoom in.